Final Report

UNIVERSITY OF CALIFORNIA

Santa Barbara

Quantitative Assessment of Remote Sensing Capabilities to Improve Monitoring of Giant Kelp Condition

A Group Project submitted in partial satisfaction of the requirements for the degree

of Master of Environmental Science and Management

for the

Bren School of Environmental Science & Management

by

EMILIE LENOIR
MICHELLE MORENO
CHARLES O'CONNOR IV
TANVI SHAH
DANIELLE TURNER

Faculty adviser:
Prof. HUNTER S. LENIHAN
Project Advisers:
Prof. ALEX PHILLIPS
Dr. TOM BELL

Project Client:
Dr. Kyle Emery
Santa Barbara Coastal Long Term Ecological Research program (SBC-LTER)

March 2026

Objectives

This project advances the use of remote sensing to monitor giant kelp (*Macrocystis pyrifera*) forest ecosystems, which provide a variety of ecosystem services, including carbon cycling and the maintenance of biodiversity. Many kelp forest ecosystem services are linked to productivity and physiological condition of kelp plants. Kelp forest monitoring data has traditionally been gathered and assessed from *in-situ* sampling by researchers using boats and scuba divers. The advance of remote sensing technology through satellites and drones has increased the capacity and reduced the costs of some kelp forest monitoring, such as canopy surface area. Satellites capture spatially broad extents of kelp forest canopy for a low-cost, while unmanned aerial vehicles (UAVs) offer high-resolution imagery at local scales. Although UAVs are well established in terrestrial ecology, their application in marine environments, particularly for submerged and floating vegetation such as kelp, remains underexplored. The Santa Barbara Coastal Long Term Ecological Research program (SBC-LTER) at UC Santa Barbara seeks to leverage this emerging technology to improve data collection, ecological monitoring, and to help inform coastal management decision-making. A key priority for the SBC-LTER is to reduce the time and cost of monitoring the physiological condition of giant kelp, which is assessed through relatively expensive laboratory analyses of diver-collected samples. The project objectives were as follows:

1. Establish Remote Sensing-Derived Indicators of Kelp Condition

We investigated quantitative relationships between remotely-sensed data and in-situ field measurements of kelp tissue nitrogen concentration, which are a key proxy for giant kelp physiological conditions. We leveraged these relationships to develop predictive models that allow researchers to assess kelp condition remotely, in particular to evaluate physiological condition, information that can be used by the mariculture industry to monitor overall kelp health and to optimize kelp harvesting.

2. Comparison Study of UAV Imagery and Satellite Imagery for Kelp Monitoring

We compared UAV imagery and Sentinel-2 satellite imagery to evaluate whether the higher spatial resolution and on-demand collection and use of UAV data provides added value for assessing kelp condition. Using consistent analytical workflows across platforms, we assessed the different monitoring strategies by determining when drone-based surveys offer meaningful advantages over publicly available satellite imagery.

Quantitative statistical models of remotely-sensed spectral indices, diver-collected kelp condition proxies, and various oceanographic metrics were used to assess how well UAV and satellite indices characterize laboratory derived kelp condition measurements. Results will help streamline and improve SBC-LTER's kelp forest monitoring effort, and may provide tools to enhance kelp harvesting productivity.

We qualitatively evaluated UAV and satellite imagery based on operational and environmental factors, including seasonality, cloud cover, tidal state, site accessibility, and temporal control. This assessment highlights the practical strengths and limitations of each method for monitoring kelp under varying conditions.

3. Investigate opportunities for complementary kelp monitoring approaches

Building on our statistical modeling, we identified opportunities where UAV technology can best complement or enhance existing satellite and diver-based monitoring. We also evaluated the tradeoffs among these monitoring approaches and assess when it is most effective to apply each method across seasons and environmental conditions to improve year-round kelp monitoring.

4. Comprehensive Literature Analysis

We conducted a comprehensive literature review to identify metrics that represent kelp conditions and evaluate current monitoring approaches. Our review assessed which remote sensing methods effectively capture kelp conditions, which metrics serve as reliable proxies, and how prior studies align with this project in terms of data types, temporal coverage, spatial scale, kelp species, and analytical methods. Studies of kelp assessments across natural, aquaculture, and restoration reefs using remotely sensed surveys were synthesized to (1) consolidate old and new data that define comparable metrics of kelp condition and the ability of remote sensing tools to assess those metrics, and (2) establish the novelty of our project (Appendix VI, Table 2).

Significance of the Project

Kelp forests provide critical habitat for a diversity of marine species, protect coastlines, and contribute to carbon sequestration (Spillias et al. 2024). These iconic ecosystems are increasingly vulnerable to climate-driven stressors such as storms, marine heat waves, and ocean acidification, as well as pollution and overgrazing, which lead to kelp forest degradation in regions like the Santa Barbara Channel. Conservation and restoration of kelp forests require timely and high-resolution survey methods that can be used in monitoring programs designed to detect early signs of ecological stress and support effective interventions (Tait, Orchard, and Schiel 2021).

Our project aims to contribute to the emerging field of UAV-assisted marine monitoring by assessing the use of remote sensing tools to track kelp canopy coverage and indicate kelp condition. Traditional monitoring techniques using satellite imagery and diver surveys are often time-consuming and/or lack the resolution to detect fine-scale changes. Monitoring through UAVs offers a flexible, cost-effective, and scalable solution that supports adaptive management and timely response to environmental threats. Our project aims to bridge the gap between technological innovation and practical marine management. By validating UAV-derived imagery

with biological field data, our project enhances the ecological interpretability of UAV-collected data thereby benefiting conservationists, aquaculturists, researchers, and policymakers aiming to safeguard and restore kelp ecosystems in California.

A major outcome of our project is the development of a reliable remote sensing-based monitoring framework that can accurately detect changes in kelp canopy coverage and correlate these changes with ecological indicators of kelp forest condition. By integrating high-resolution aerial imagery with field-based biological data, we identified actionable insights to support more informed and responsive kelp recovery strategies. Beyond kelp forests, our project also highlights the broader potential of UAV technology as a versatile tool for marine conservation, restoration, and aquaculture practices, offering scalable, cost-effective solutions for monitoring and managing coastal ecosystems.

Background and Literature Review

Kelp Forest Ecology and Environmental Drivers of Kelp Condition

Giant kelp (*Macrocystis pyrifera*) thrives under high light as well as the relatively low temperatures and high nutrient concentrations that are found in coastal upwelling regions (Bell and Siegel 2021). Giant kelp exhibits rapid population and thus biomass turnover, allowing kelp forests to respond quickly to environmental change, such as the onset of upwelling. New fronds continuously replace those lost to senescence, which is primarily age-dependent but also influenced by physical (e.g., wave) disturbance and nutrient availability (Rodriguez et al. 2013). Reproductive spores are produced year-round, and recruitment occurs when sufficient reef space and light are available. Under ideal conditions, giant kelp can grow up to 20 m tall and increase in length by as much as 60 cm per day. Early life stages have high light requirements and are vulnerable to intraspecific shading. Consequently, higher light availability along canopy edges promotes recruitment, while senescence progresses outward from the canopy interior (Bell & Siegel, 2021).

Giant kelp growth is closely linked to seasonal variation in seawater nitrate concentrations. Growth is most rapid during cool, nutrient-rich upwelling periods and declines during warm, nutrient-poor conditions. In southern California, growth is fastest in winter and spring, when nutrients are abundant and competition for light and space is low, and slowest in summer and early fall, when nutrient limitation and canopy competition increase (Bell et al. 2020).

Physiological conditions vary in parallel with these seasonal upwelling dynamics. Bell and Siegel (2022) showed that the chlorophyll a to carbon ratio (Chl:C), a proxy for physiological condition, is positively associated with kelp growth rate, frond initiation, and biomass accumulation. In turn, Chl:C is positively related to seawater nitrate concentrations and correlated with changes in canopy biomass in southern California. Seasonal declines in Chl:C precede reductions in net primary production later in the year.

Beyond seasonal weather forcing, kelp canopy biomass is influenced by wave disturbance, nitrate availability, and the North Pacific Gyre Oscillation (NPGO), with their relative importance varying spatially (Bell et al., 2015). Wave disturbance is a dominant driver of kelp mortality and therefore abundance along the more exposed central California coast, while nitrate availability is more strongly associated with kelp growth and thus biomass at protected sites. Positive values of the NPGO index are linked to increased nitrate availability and higher kelp biomass (Bell et al. 2015).

Biotic interactions further regulate kelp abundance. Higher sea urchin densities are associated with reduced canopy biomass and were the dominant correlate at 25% of southern California sites with long-term urchin records (Guenther et al. 2012). In contrast, urchin density was not an important driver in central California where sea otters are prevalent (Bell et al., 2015). Grazing pressure increases when storms or warm, nutrient-poor conditions reduce drift algae, intensifying herbivory. Human activities can amplify these effects: fishing can weaken top-down control of grazers, contributing to kelp loss, while direct removal of sea urchins has supported kelp recovery (Foster and Schiel 2010). Degraded water quality and El Niño Southern Oscillation (ENSO) events also contribute to kelp declines and may indirectly increase grazing pressure by reducing drift algal supply (Foster & Schiel, 2010).

Climate-Driven Threats to Kelp Condition

Temperate coastal ecosystems and their flora and fauna are highly sensitive to warming events. With continued ocean warming, projections indicate declines in marine biomass at all trophic levels and reduced primary production. Kelp forest primary production is particularly important because it provides physical structure and habitat and food resources to many species (Miller, Reed, and Brzezinski 2010). The nutritional content of macroalgae affects feeding preferences, consumption rates, and physiological performance of algal consumers. Greater mean values of the C:N ratio in the 19-year period (2002 through 2021) of SBC-LTER time series data were present between the warmer months of August and November, while smaller values were present during the upwelling season, between March and June. The C:N values in giant kelp blade tissue are significantly positively correlated with seawater temperature.

Nutritional content of giant kelp appears to decline significantly with warming, which may also be a result of giant kelp's inability to store nitrogen reserves for longer than approximately three weeks (Lowman et al. 2022) . This could have implications for kelp forest food webs in the Santa Barbara Channel as well as for the food webs of recipient ecosystems that rely on exported kelp. Compensatory feeding by consumers is an additional concern, as decreased nutritional quality may lead to consumption of a greater quantity of the same food to compensate. This can change the state of an entire ecosystem, as seen with shifts from a kelp forest into an urchin barren.

To conclude, results suggest that giant kelp, a highly productive foundation species that supports biodiverse coastal ecosystems, has experienced a nearly 45% decline in the nutritional quality of blade tissue between 2002 and 2021 (Lowman et al., 2022).

Regional Context: Santa Barbara Channel Kelp Forest Dynamics

Response of kelp biomass to environmental conditions varies among different subregions of the Santa Barbara Channel. This region has high spatial variability of nutrients, with cooler, nutrient-rich conditions from upwelling present in western portion of the Channel, and warmer, more nutrient-limited conditions in the eastern portion. Spatial variability in wave exposure is also dramatic, with some areas of the coastline sheltered from swells, while others are directly exposed. Winter storms in the North Pacific create large swell waves (> 4 m) and summer months see a mixture of smaller wave heights (< 3 m). The central coast of California (Año Nuevo to Point Conception) is more exposed to westerly and north-westerly swells as a result of its orientation, whereas the southern California mainland coast (Point Conception to the USA/Mexico border) has a range of wave exposures as a result of variable coastline orientations as well as the presence of the Channel Islands (Bell et al., 2015).

Coastal upwelling is most prominent in the spring and brings nutrient-rich, colder waters to the coastal shelf. Upwelling is less intense and more intermittent in southern California, with low nutrient levels during the summer. Populations of giant kelp in California are extremely dynamic and highly susceptible to removal by ocean waves. Entire forests may be destroyed during one single storm but can fully recover in 1-2 years following the destruction (Bell et al., 2015).

Winter losses of regional kelp canopy biomass are positively correlated with significant wave height, while spring recoveries are negatively correlated with sea surface temperature. Longer period, lower-frequency, cycles in kelp biomass correspond to the North Pacific Gyre Oscillation (NPGO), waves, and nutrients levels but have about a 3-year lag (Di Lorenzo et al. 2008; Cavanaugh et al. 2011). This lag is suspected to be related to recruitment and mortality of entire plants, which happens more episodically than loss of fronds. The NPGO is driven by variations in wind-driven upwelling and horizontal advection. It corresponds with ecosystem productivity in nutrient levels and chlorophyll concentrations. Previous studies showing fluctuation in kelp abundance cycles of 3 to 5 years have suggested it results from seasonal forcings, like wave disturbance. Overall, there is a large amount of regional heterogeneity in the response of kelp biomass to environmental factors (Cavanaugh et al., 2011).

The environmental drivers of kelp biomass vary on an interannual-to-decadal timescales, making system responses difficult to predict. The rapid response of kelp to environmental stressors, combined with spatial and temporal variability in the Santa Barbara Channel, underscores the need for monitoring approaches that can detect fine-scale changes in kelp condition across coastal environments.

Spectral Indices for Assessing Kelp Condition

A key component of this project focused on investigating spectral indices that can help inform kelp nutrient levels, productivity, and in general reduce labor-intensive monitoring efforts through the use of remote sensing. In terrestrial environments, the Normalized Difference Vegetation Index (NDVI) is a useful indicator of terrestrial greenness. Several studies have investigated applications of NDVI for monitoring kelp canopy. Past work has developed correlations with chlorophyll a and NDVI (Chadwick et al. 2024), as well as with biomass and NDVI (Cavanaugh et al. 2010). These correlations are particularly relevant given the established relationships between Chl:C ratios and kelp growth rates, suggesting that spectral indices may provide a means to remotely assess the physiological condition indicators discussed earlier.

Prior studies have investigated the detection of submerged kelp through different spectral indices using hyperspectral data. Timer et al. (2022) reported that submerged kelp generated a higher reflectance in the red-edge band, while kelp at the surface had a high reflectance in near-infrared. Figure 1 shows the wavelengths of red-edge and near-infrared bands in hyperspectral data.

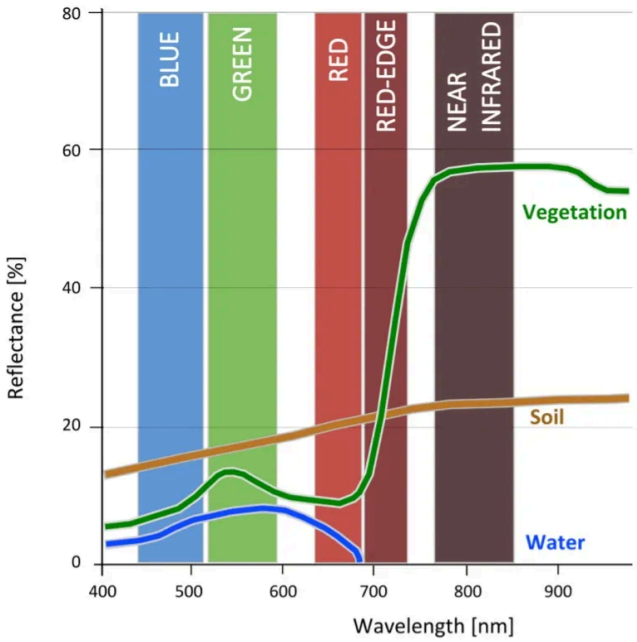

Figure 1. Wavelengths in hyperspectral data (Reference: RapidEye Whitepaper).

While spectral indices applied directly to kelp can be useful and informative, kelp conditions may be inferred through other proxies. Snyder et al. (2020) examined the development of a "kelp stress index" using satellite-derived temperature data, in-situ measurements, and models of nitrate flux (2020). They found that a daily measurement, at a spatial resolution of 1 km, provided the optimal combination to inform the stress index.

These studies of remotely-sensed metrics of kelp condition indicate that there may be opportunity for pairing multispectral data with *in-situ* measurements and laboratory analyses to develop remotely accessed proxies for kelp condition.

Remote Sensing Applications for Kelp Conservation and Management

Aquaculture and kelp restoration managers can benefit from remote sensing in a variety of innovative and convenient ways. The primary benefit of remote sensing is allowing managers and their team to map dangerous, inconvenient, or inaccessible locations, such as remote islands, heavily polluted waters, or cave systems. This allows kelp restoration and aquaculture managers to access areas along the coastline or coastal bluffs without risking damage to delicate ecosystems or disturbance to marine and coastal wildlife.

An issue of concern for managers using UAVs for kelp restoration and aquaculture is their vulnerability to wind speed, rain, fog, and sun glare. Wind speeds are notably higher along the coastline and ocean, which makes it impractical to use UAVs in windy weather conditions. Similarly, UAV imaging is limited to the time of day as the reflectivity of the sun on the ocean surface is important to factor into UAV imaging for usable, high-quality data (Cunliffe et al. 2021). However, the nature of UAVs needing little pre-flight preparation makes it easy to reschedule coastal flights to avoid poor weather conditions.

Another challenge for managers is camera angles on drones (Young et al. 2022). Certain angles can cause the cameras and lidar systems of drones to vastly warp the sizes of a measured species/area. This issue could become further exacerbated by the time of day or wind speed of the area, which may restrict certain angles that traditionally minimize camera angle distortions.

While existing studies demonstrate the potential of remote sensing for kelp monitoring, a gap remains in developing validated, high-resolution UAV frameworks that integrate canopy coverage metrics with field-based assessments of ecological condition at management-relevant scales. By pairing UAV-derived imagery with *in-situ* measurements of biological indicators such as nutrient content, growth rates, and biomass, it becomes possible to translate remotely-sensed canopy characteristics into ecologically meaningful assessments of kelp forest health. This approach bridges technological capabilities with the practical information needs of conservation managers, restoration practitioners, and policymakers working to protect and restore kelp ecosystems.

Methods

To determine whether kelp condition can be sensed remotely, we divided our project into two complementary components, a drone-based study and a satellite-based study. Each component included two analytical workflows and was guided by an ongoing data and literature synthesis aimed at identifying existing research on kelp remote sensing, evaluating

which indices most effectively estimate kelp condition, and assessing whether previous studies have incorporated time-series or diver data.

Below, we outline the data processing methods used for both studies. Each study requires image classification (workflow 1) and spectral indices analysis (workflow 2). The ArcGIS steps for both are described in detail in Appendix II.

Drone Image Processing:

For Workflow 1, we used drone imagery provided by the SBC LTER program. The imagery was stitched into orthomosaics by Dr. Tom Bell at Woods Hole Oceanographic Institution. We processed these images in ArcGIS Pro to produce a Normalized Difference Vegetation Index (NDVI) layer and a Normalized Difference Red-Edge (NDRE) layer, distinguishing vegetation from non-vegetated areas. From this output, we generated a kelp polygon layer to represent the spatial extent of kelp canopies. These polygons served as the basis for Workflow 2, in which we extracted and summarized index values corresponding specifically to the kelp extent.

Satellite Image Processing:

We acquired Sentinel-2 imagery using the Copernicus Data Space Browser. Navigating to the Sentinel-2 Data Explorer, we located the study area (either Arroyo Quemado Reef or Mohawk Reef) and inspected it using True Color and False Color visualizations to ensure clear conditions and visible kelp canopy. When available, we downloaded satellite imagery within one day of each drone survey date; otherwise, satellite imagery downloaded was within +/- two weeks from survey dates. Spectral bands 2 through 8A were imported into ArcGIS Pro for analysis. Workflow 1 produced a NDVI layer and an 8-band layer within the classified kelp extent to be used in Workflow 2 to calculate mean satellite index values.

The final product of the drone and satellite ArcGIS Pro Workflows was a comprehensive data table linking remotely sensed kelp condition metrics (NDVI and NDRE) with LTER kelp physiological data from diver surveys. This integrated dataset was analyzed in R as detailed in the Statistical Analyses & Discussion section of this report. See Table 1 for the formulas used to calculate each index.

Table 1. Remotely Sensed Indices

Index	Equation
Normalized Difference Vegetation Index (NDVI)	NDVI = (NIR - R) / (NIR + R)
Normalized Difference Red-Edge (NDRE)	NDRE = (NIR - RE) / (NIR + RE)

Statistical Analyses

We used generalized additive models (GAMs) for our analyses because relationships between kelp condition and spectral indices were nonlinear based on our preliminary tests. GAMs estimate smooth functions of predictor variables, allowing flexible nonlinear fits while maintaining interpretability.

We used leave-one-out cross-validation (LOOCV) to evaluate predictive performance and overfitting of the GAMs. LOOCV is a resampling technique in which each observation is iteratively left out of the training set and used for validation ("Leave One Out Cross-Validation"). LOOCV is particularly useful when training data is limited because it maximizes the use of training data. Each observation was withheld once as a test case, while the remainder of the data was used to train the model. This process was repeated 22 times, corresponding to the dataset sample size. The R^2 value was computed for each iteration and averaged to obtain the LOOCV R^2 (Ballcando and Taylor, 2022).

Given our relatively small dataset, LOOCV R^2 is a more accurate metric of prediction performance compared to R^2 obtained from the full models. The model selection process is based on comparisons of LOOCV R^2, and the full model R^2 presented for the top-performing models.

The following questions guide the model selection process.

1) Which metric—C:N ratio or % Nitrogen—is easier to predict from remote sensing data?

We first determined which response variable, carbon-to-nitrogen ratio (C:N) and percent nitrogen by mass (%N), is easier to predict. We evaluated both options in consultation with Dr. Kyle Emery and Dr. Robert Miller and with reference to the literature. We selected %N as the primary proxy because it is more directly linked to kelp net primary production and varies meaningfully across most kelp systems (Bell et al. 2018). Carbon content, by contrast, is relatively stable globally, making C:N less broadly applicable (Reed et al. 2015). The Santa Barbara Channel and other strong upwelling regions are a notable expectation. During upwelling events, pulses of CO2-rich deep water reach the surface, driving carbon uptake in kelp and C:N variability (Frieder et al. 2012). Though C:N is informative for Santa Barbara, %N is more broadly relevant across kelp forests globally.

Model comparisons (Figure 2) support this decision. In comparing models of the same explanatory variables, predicting %N generally produced higher full-model R^2 values compared to those predicting C:N. Accordingly, we used %N as the response variable in all subsequent analyses.

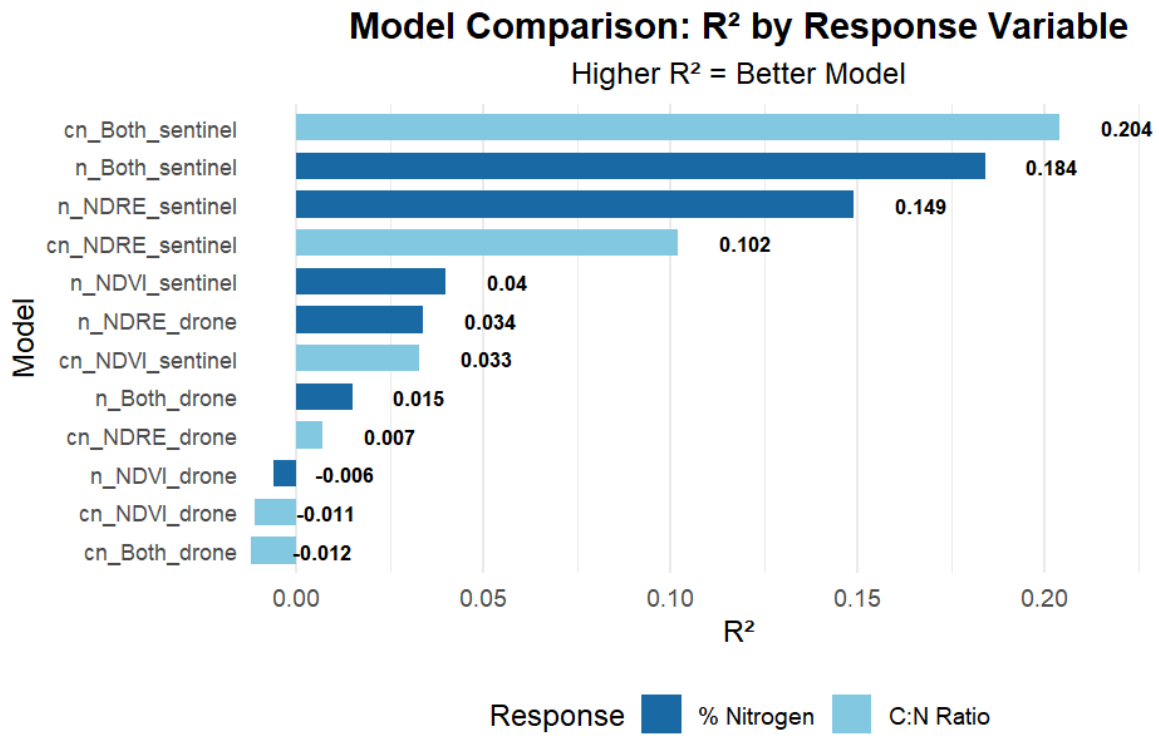

Figure 2. A comparison of full-model R^2 values for GAMs with varying response variables (%N and C:N ratio) predicting kelp condition, across all combinations of remote sensing index (NDVI, NDRE, and Both) and platform (Drone and Sentinel). Higher R^2 values indicate better model fit. Overall, %N models outperformed C:N models, though the highest performing model is %N with using both Sentinel variables to predict C:N. Sentinel models outperformed every corresponding drone model.

2) Which remotely sensed variables are valuable for predicting kelp condition?

We next evaluated whether NDVI, NDRE, or both produced the strongest predictive models. As shown in Figure 3, amongst drone models, the NDRE-only model achieved the highest LOOCV R^2 values. Amongst sentinel models, the model combining NDVI and NDRE performed the best.

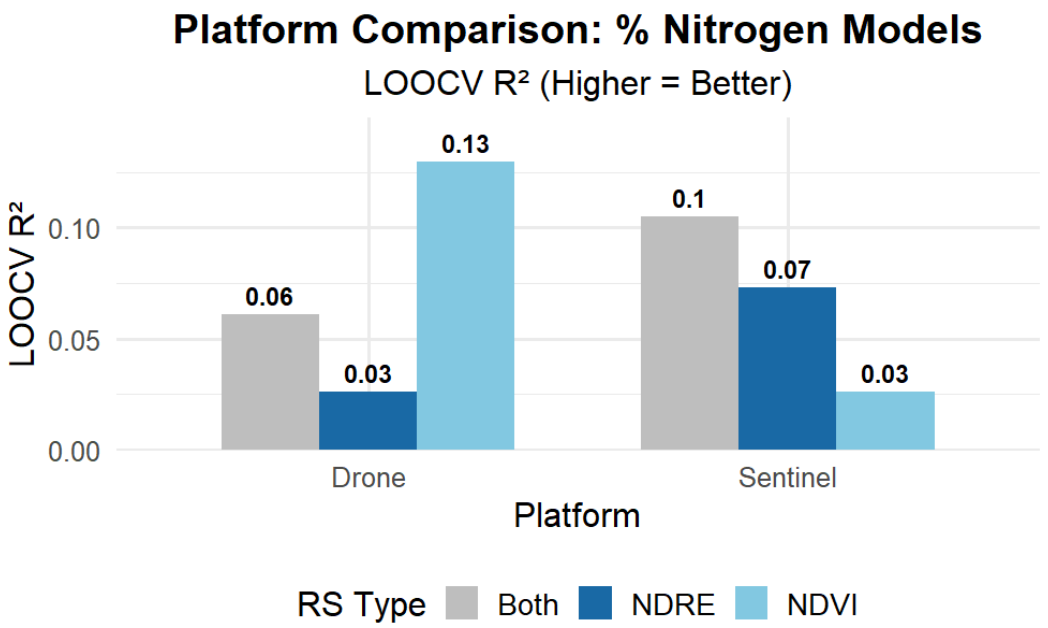

Figure 3. Comparison of LOOCV R^2 for GAM models with varying remotely sensed indices.

3) Does including oceanographic data improve model performance?

Because oceanographic factors influence regional nitrate concentrations, we added oceanographic data to each model to determine if this improved overall performance and changed relative performance between models. We selected North Pacific Gyre Oscillation (NPGO), Biologically Effective Upwelling Transport Index (BEUTI) and El Nino Southern Oscillation (ENSO) due to their ecological significance and motivation from prior studies. In Bell et al. 2015 and Lowman et al. 2022, these metrics proved to be strong predictors of kelp condition.

Below, we present a comparison of models including different oceanographic metrics. Notably, index performance shifted when we included BEUTI. Sentinel NDVI models improved substantially with BEUTI, outperforming NDRE-only models. We interpret this to mean that NDVI may better capture environmentally driven variability (i.e., nutrient dynamics) when paired with oceanographic context. In other words, NDVI appears more informative when the model explicitly incorporates broader productivity signals.

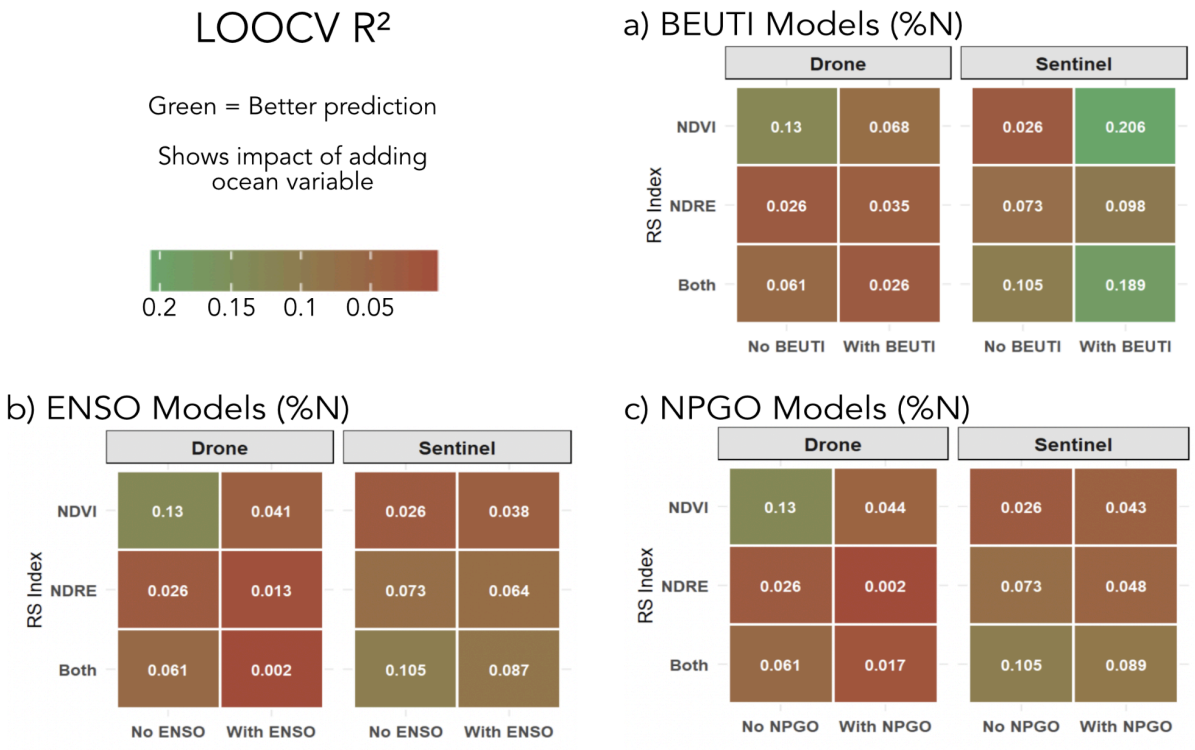

Figure 4. Leave One Out Cross Validation (LOOCV) R^2 of models with and without oceanographic data. LOOCV R^2 values are shown for models predicting kelp %N across three remote sensing indices (NDVI, NDRE, and Both) and two platforms (Drone and Sentinel). Plot A displays models with and without the inclusion of BEUTI as an oceanographic covariate; plot B with and without the inclusion of ENSO as an oceanographic covariate; and plot C with and without NPGO as an oceanographic covariate. Higher R^2 values (green) show better model performance.

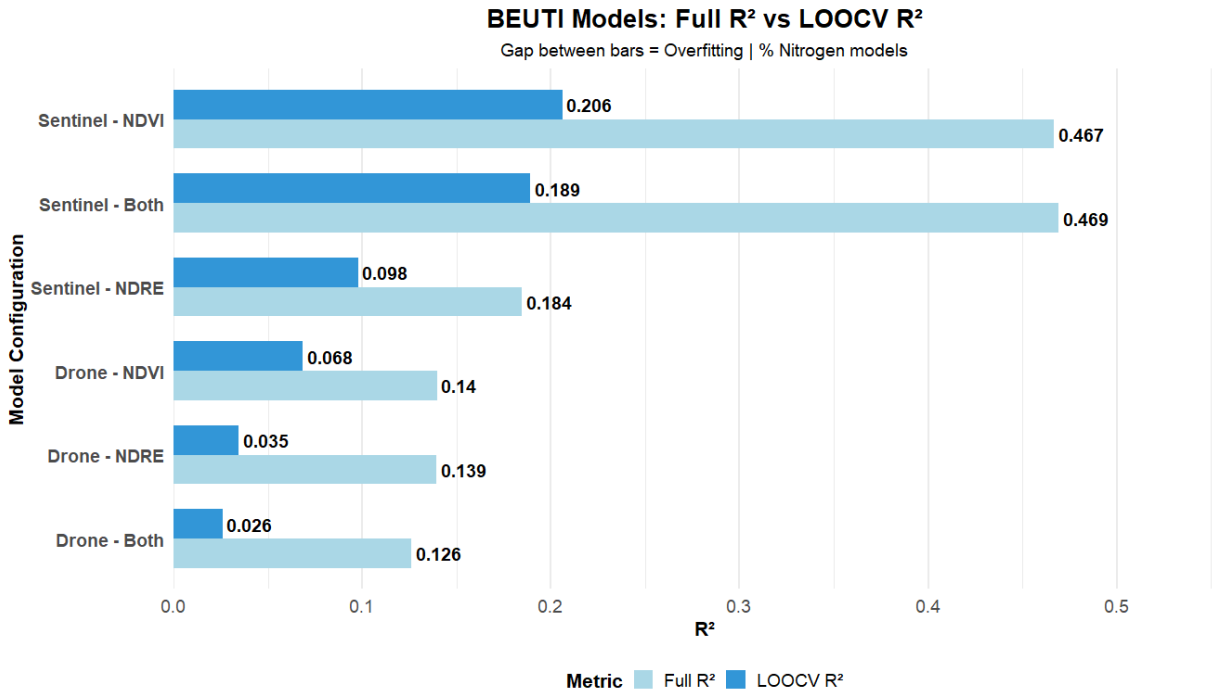

Figure 5. BEUTI-only model comparison of LOOCV R and full model shows significant overfitting. Looking at the best performing models (Sentinel NDVI and Sentinel Both), the full model performs well (R2 ~ 0.5), indicating that the model fits well to the data. However, when tested for prediction using LOOCV, the model performs much worse (LOOCV R2 ~0.2).

Based on a comparison of LOOCV R^2 across all models, we selected Sentinel NDVI + BEUTI ~ %N as our final model (LOOCV R^2 = 0.206). This model substantially outperformed models using NPGO (best R^2 = 0.089) or ENSO (best R^2 = 0.105). The model explains 20.6% of variance when predicting kelp nitrogen content on unseen samples.

Figure 5 shows that the best models (Sentinel NDVI + BEUTI ~ %N and Sentinel Both + BEUTI ~ %N) have an R2 ~ 0.5, but the LOOCV R2 drops to ~0.2 This gap indicates that the best models are overfitting on the data. Overfitting is caused by model complexity and small sample size. In this case, we expect this limitation could be overcome by increasing the sample size as the highest performing model (Sentinel NDVI + BEUTI ~ %N) only includes 2 predictor variables.

4) How does a predictive model built using satellite data compare with a model built using drone data?

Comparisons across platforms (Figure 5) show that satellite-based models generally outperformed drone-based models. These results prompted us to examine whether higher spatial resolution imagery may reduce model performance. Drone and satellite imagery captures spatial variability on different scales within kelp beds, whereas ground-truth %N measurements are collected by divers along a single transect at each reef. Due to this spatial

scale mismatch, high-resolution imagery that incorporates greater within-bed variability may generate predictions that are representative of the full canopy extent, rather than at the transect line. This hypothesis assumes that the transect line is not representative of the normalized conditions in the canopy bed, so that increased variance across the canopy bed would increase the mismatch between overall canopy condition and transect line condition.

To evaluate this hypothesis, we quantified prediction error as the difference between observed and predicted %N for each sampling unit. We chose the highest performing models for drone and sentinel for this analysis, which used NDVI and BEUTI to predict %N. We then compared the prediction error (predicted %N - actual %N) to within-bed variance in vegetation indices (Figure 6a and 6b). If increased spatial variance reduces model performance, we would expect prediction error to increase with increasing variance.

These figures show that spatial variance in NDVI actually does not have a significant relationship with prediction error. This is evident via the lack of a clear trend between variance (x-axis) and error (y-axis) and from the high p-values, where $p > 0.05$ indicates no statistically significant relationship. With this result, we expect that environmental factors that affect aerial image quality may drive the model error. For example, sea surface roughness could affect the drone and satellite NDRE and NDVI indices. This hypothesis could be investigated by including the Beaufort scale in the predictive model, which captures wind-driven ocean conditions. Exploratory comparisons between drone and satellite measurements further confirmed different scales of spatial variability, which may contribute to variation in predictive performance (Appendix I, Figures 11 and 12).

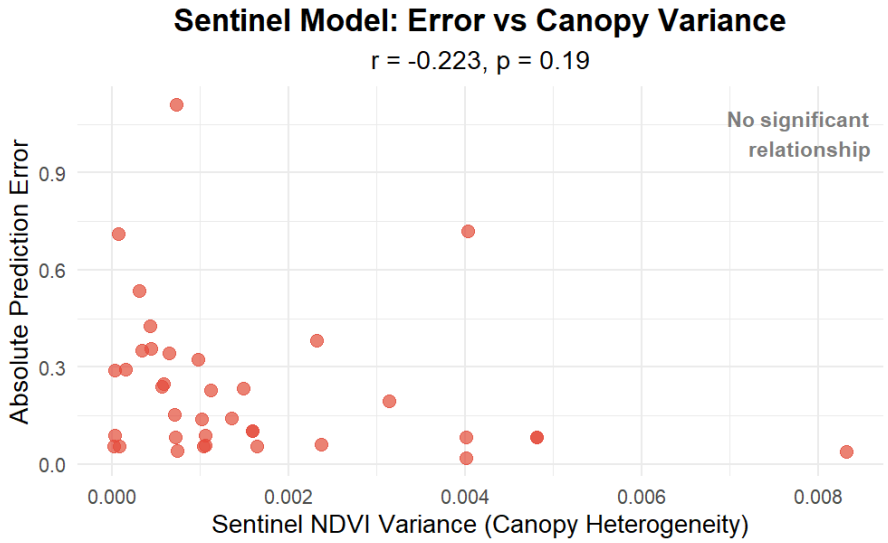

Figure 6a. Comparison of Sentinel Model Error to Sentinel Canopy Variance in NDVI.

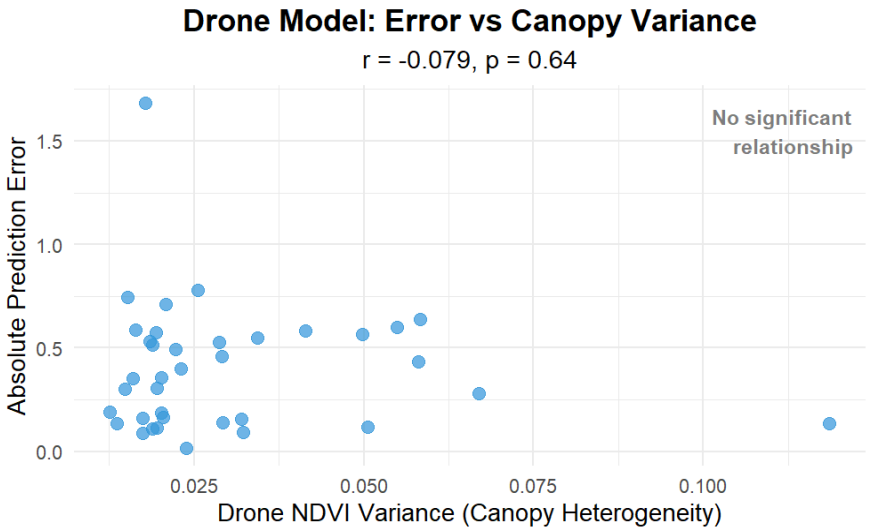

Figure 6b. Comparison of Drone Model Error to Drone Canopy Variance in NDVI.

Discussion

This study demonstrates that kelp physiological condition can be estimated remotely with reasonable accuracy, with %N emerging as a more reliable response variable than C:N. Models using %N consistently outperformed those using C:N, reflecting the relative stability of carbon content in giant kelp tissue compared to the rapid, environmentally driven variability of nitrogen. Because %N is closely linked to net primary production and growth rates, it serves as a stronger ecological proxy for kelp condition than C:N and our results confirm it is also the better-performing response variable.

Across platforms, GAMs identified NDVI as the most informative spectral signal. NDVI alone, without oceanographic metrics, provided the best-performing models for UAV data. Satellite-based models benefited from the combined use of NDVI and BEUTI (Figure 4c). The models show that satellite-based approaches outperform drone-based approaches. Including environmental covariates generally increased model complexity without benefit, with the exception of BEUTI (Figure 4c).

Diver surveys generate accurate measurements of kelp condition but can be constrained by access, environmental conditions, safety, and logistical requirements. Both satellite and UAV imagery offer effective alternatives for monitoring kelp reefs that are difficult or infeasible to survey by divers *in situ*. Satellite data enable broad spatial coverage and repeated observations across large coastal areas, while UAV surveys provide high-resolution, flexible data collection that can be deployed around cloud cover or targeted to specific sites. Together, diver, satellite, and UAV approaches support a complementary monitoring strategy in which each method is applied based on environmental conditions, accessibility, and monitoring objectives, strengthening overall assessments of kelp condition.

Implications

Our findings carry important ecological and applied implications. Many important commercial species, such as sea urchins, rockfish, and abalone, depend directly on kelp forests for food and habitat. Remote sensing of kelp condition can inform fisheries management by forecasting recruitment success, identifying critical habitat, and tracking post-disturbance recovery trajectories. This helps managers designate marine protected areas, adjust fishing effort to protect certain habitat, and set harvest limits following environmental disturbances.

For kelp aquaculture operations, %N is a critical quality metric linked to nutritional value and market applications like determining optimal harvest timing (i.e., a high %N is valuable for feed and fertilizer applications). Remote sensing frameworks that predict tissue nitrogen content enable aquaculturists to schedule harvests strategically when tissue quality peaks, typically following upwelling events.

The ability to remotely estimate %N gives researchers and managers a tool for assessing kelp condition and tracking kelp condition over time, which enables proactive interventions, such as urchin removal or targeted restoration efforts, rather than reactive responses after forests have collapsed. Healthy kelp forests support greater biodiversity by providing habitat structure and nutritious food resources. For this reason, kelp forest condition can also be used as an indicator for broader ecosystem function.

As climate change intensifies marine heat waves, alters upwelling patterns, and increases storm frequency, long-term monitoring of kelp condition becomes essential for understanding kelp responses and informing adaptation strategies. Remote sensing time series can reveal whether kelp %N is declining on decadal timescales or whether forests show resilience and the capacity to recover.

Beyond direct resource management, remote sensing of kelp condition has implications for coastal resilience planning and for industries such as ecotourism, which depend on healthy, visually intact reef ecosystems. This enhances public engagement and can be integrated into regulatory frameworks for permitting and compliance monitoring of kelp harvest and aquaculture operations.

The methodological framework developed here is transferable beyond the Santa Barbara Channel and the SBC-LTER. While specific model coefficients may require calibration, the approach can be applied to other California kelp forests, different kelp species, and kelp ecosystems globally. This positions remote sensing as a scalable tool for tracking changes in kelp canopy cover, reef stability, and post-disturbance recovery.

Together, these implications underscore the value of integrating ecological field data with remote sensing technologies to advance fisheries management, aquaculture, conservation,

climate adaptation, and coastal management. By providing frequent, broad-scale assessments of kelp physiological condition, this approach enables more informed and timely decision-making to safeguard kelp ecosystems and the communities that depend on them.

References

About—Kelp-O-Matic. (n.d.). *Kelp-O-Matic documentation*. Retrieved January 10, 2025, from https://kelp-o-matic.readthedocs.io/en/stable/about/

Ballacando, S., Taylor J. *Leave one out cross-validation (LOOCV)*. Stanford University. https://web.stanford.edu/class/stats202/notes/Resampling/LOOCV.html

Bell, T. W., Cavanaugh, K. C., Reed, D. C. and Siegel, D. A. (2015), Geographical variability in the controls of giant kelp biomass dynamics. J. Biogeogr., 42: 2010-2021. https://doi.org/10.1111/jbi.12550

Bell, T. W., Cavanaugh, K. C., & Hockridge, E. G. (2021). An automated method for mapping giant kelp canopy dynamics from UAV. Frontiers in Environmental Science, 8, 587354. https://doi.org/10.3389/fenvs.2020.587354

Bell, T. W., Cavanaugh, K. C., Saccomanno, V. R., Cavanaugh, K. C., Houskeeper, H. F., Eddy, N., Schuetzenmeister, F., Rindlaub, N., & Gleason, M. (2023). Kelpwatch: A new visualization and analysis tool to explore kelp canopy dynamics reveals variable response to and recovery from marine heatwaves. *PLOS ONE, 18*(3), e0271477. https://doi.org/10.1371/journal.pone.0271477

Bell, T. W., Cavanaugh, K. C., Siegel, D. A., Nidzieko, N. J., & Cavanaugh, K. C. (2020). The utility of satellites and autonomous remote sensing platforms for monitoring offshore aquaculture farms: A case study for canopy forming kelps. *Frontiers in Marine Science, 7*, 520223. https://doi.org/10.3389/fmars.2020.520223

Bell, T. W., Reed, D. C., Nelson, N. B. and Siegel, D. A. (2018), Regional patterns of physiological condition determine giant kelp net primary production dynamics. Limnol. Oceanogr., 63: 472-483. https://doi.org/10.1002/lno.10753

Bell, T. W., & Siegel, D. A. (2021). Nutrient availability and senescence spatially structure the dynamics of a foundation species. *Proceedings of the National Academy of Sciences of the United States of America* 119(1):e2105135118. doi:10.1073/pnas.2105135118

Belmonte, A., Sankey, T., Biederman, J.A., Bradford, J., Goetz, S. J., Kolb, T., & Woolley, T. (2020). UAV-derived estimates of forest structure to inform ponderosa pine forest restoration. *Remote Sensing in Ecology and Conservation, 6*(2), 181–197. https://doi.org/10.1002/rse2.137

Cavanaugh, K. C., Cavanaugh, K. C., Bell, T. W., & Hockridge, E. G. (2021). An automated method for mapping giant kelp canopy dynamics from UAV. *Frontiers in Environmental Science, 8*, 587354. https://doi.org/10.3389/fenvs.2020.587354

Cavanaugh, K. C., Siegel, D. A., Kinlan, B. P., & Reed, D. C. (2010). Scaling giant kelp field measurements to regional scales using satellite observations. *Marine Ecology Progress Series, 403*, 13–27. https://doi.org/10.3354/meps08467

Cavanaugh, K. C., Siegel, D. A., Reed, D. C., & Dennison, P. E. (2011). Environmental controls of giant-kelp biomass in the Santa Barbara Channel, California. *Marine Ecology Progress Series, 429*, 1–17. https://doi.org/10.3354/meps09141

Chadwick, K. D., Davis, F., Miner, K. R., Pavlick, R., Reynolds, M., Townsend, P. A., & Brodrick, P. G. (2025). Unlocking ecological insights from sub-seasonal visible-to-shortwave infrared imaging spectroscopy: The SHIFT campaign. *Ecosphere, 16*(3), e70194. https://doi.org/10.1002/ecs2.70194

Di Lorenzo, E., Schneider, N., Cobb, K. M., Chhak, K., Franks, P. J. S., Miller, A. J., McWilliams, J. C., Bograd, S. J., Arango, H., Curchister E., Powell, T. M. & Rivere, P. (2008). North Pacific Gyre Oscillation links ocean climate and ecosystem change. Geophys. Res. Lett., 35, L08607, https://doi.org/10.1029/2007GL032838

Foster, M. S., & Schiel, D. R. (2010). Loss of predators and the collapse of southern California kelp forests: Alternatives, explanations, and generalizations. *Journal of Experimental Marine Biology and Ecology, 393*(1), 59–70. https://doi.org/10.1016/j.jembe.2010.07.002

Frieder, C. A., Nam, S. H., Martz, T. R., & Levin, L. A. (2012). High temporal and spatial variability of dissolved oxygen and pH in a nearshore California kelp forest. *Biogeosciences, 9*(10), 3917–3930. https://doi.org/10.5194/bg-9-3917-2012

Guenther, C. M., Lenihan, H.S., Grant, L.E., Lopez-Carr, D., & Reed, D.C. (2012). Trophic Cascades Induced by Lobster Fishing Are Not Ubiquitous in Southern California Kelp Forests. *PLOS ONE* 7(11):e49396. https://doi.org/10.1371/journal.pone.0049396

Hamilton, S. L., Gleason, M. G., Godoy, N., Eddy, N., & Grorud-Colvert, K. (2022). Ecosystem-based management for kelp forest ecosystems. *Marine Policy, 136*, 104919. https://doi.org/10.1016/j.marpol.2021.104919

Lowman, H. E., Emery, K. A., Dugan, J. E., & Miller, R. J. (2022). Nutritional quality of giant kelp declines due to warming ocean temperatures. *Oikos, 2022*(7). https://doi.org/10.1111/oik.08619

McPherson, M. L., & Kudela, R. M. (2022). Kelp patch-specific characteristics limit detection capability of rapid survey method for determining canopy biomass using an unmanned aerial vehicle. *Frontiers in Environmental Science, 10*, 690963. https://doi.org/10.3389/fenvs.2022.690963

Miller, R. J., Reed, D.C., & Brzezinski, M.A. (2010). Partitioning of primary production among giant kelp (*Macrocystis Pyrifera*), understory macroalgae, and phytoplankton on a temperate reef. https://doi.org/10.4319/lo.2011.56.1.0119

Paxton, A. B., & Freedman, R. M. (n.d.). *Untangling how kelp contributes to coastal resilience in Alaska: Literature review and community discussions*. Retrieved January 9, 2025, from https://repository.library.noaa.gov/view/noaa/61596

Reed, D. C., Carlson, C.A., Halewood, E.R., Nelson, J.C., Harrer, S.L., Rassweiler, A., & Miller, R.J. (2015). Patterns and controls of reef-scale production of dissolved organic carbon by giant kelp *Macrocystis Pyrifera*. *Limnology and Oceanography* 60(6):1996–2008.

Rodriguez, G.E., Rassweiler, A., Reed, D.C. & Holbrook, S.J. (2013), The importance of progressive senescence in the biomass dynamics of giant kelp (*Macrocystis pyrifera*). *Ecology*, 94: 1848-1858. https://doi.org/10.1890/12-1340.1

Saccomanno, V. R. (2023). Using unoccupied aerial vehicles to map and monitor changes in emergent kelp canopy after an ecological regime shift. *Remote Sensing in Ecology and Conservation*. https://doi.org/10.1002/rse2.295

Schroeder, S. B., Dupont, C., Boyer, L., Juanes, F., & Costa, M. (2019). Passive remote sensing technology for mapping bull kelp (*Nereocystis luetkeana*): A review of techniques and regional case study. *Global Ecology and Conservation, 19*, e00683. https://doi.org/10.1016/j.gecco.2019.e00683

Snyder, J. N., Bell, T. W., Siegel, D. A., Nidzieko, N. J., & Cavanaugh, K. C. (2020). Sea surface temperature imagery elucidates spatiotemporal nutrient patterns for offshore kelp aquaculture siting in the Southern California Bight. *Frontiers in Marine Science, 7*, 22. https://doi.org/10.3389/fmars.2020.00022

Spillias, S., Cottrell, R.S., Layton, C., O'Brien, K.R. & McDonald-Madden, E. (2024). Having our kelp and eating it too: Minimizing trade-offs from seaweed farming. *Journal of Cleaner Production* 448:141150. doi:10.1016/j.jclepro.2024.141150

Tait, Leigh W., Shane Orchard, and David R. Schiel. 2021. Missing the forest and the trees: Utility, limits and caveats for drone imaging of coastal marine ecosystems. *Remote Sensing* 13(16):3136. doi:10.3390/rs13163136.

Timmer, B., Reshitnyk, L. Y., Hessing-Lewis, M., Juanes, F., & Costa, M. (2022). Comparing the use of red-edge and near-infrared wavelength ranges for detecting submerged kelp canopy. *Remote Sensing*, 14(9), 2241. https://www.mdpi.com/2072-4292/14/9/2241

Appendix

I. Exploratory Data Analysis

Linear Regression Analysis

```
Residuals:
   Min     1Q Median     3Q    Max
-81161  -6644    7201  21840  36996

Coefficients:
                   Estimate Std. Error t value Pr(>|t|)
(Intercept)         -31142      21172  -1.471   0.1490
Drone.mean.NDVI      30837      39371   0.783   0.4380
Drone.mean.NDRE      70954      40438   1.755   0.0868 .
Sentinel.mean.NDVI  245791     111881   2.197   0.0337 *
Sentinel.mean.NDRE -212607     169816  -1.252   0.2177
---
Signif. codes:  0 ‘***’ 0.001 ‘**’ 0.01 ‘*’ 0.05 ‘.’ 0.1 ‘ ’ 1

Residual standard error: 32750 on 41 degrees of freedom
Multiple R-squared:  0.2589,    Adjusted R-squared:  0.1866
F-statistic:  3.58 on 4 and 41 DF,  p-value: 0.01357
```

Figure 7. Output of the exploratory multiple linear regression for Drone and Satellite NDRE + NDVI on Nitrogen %.

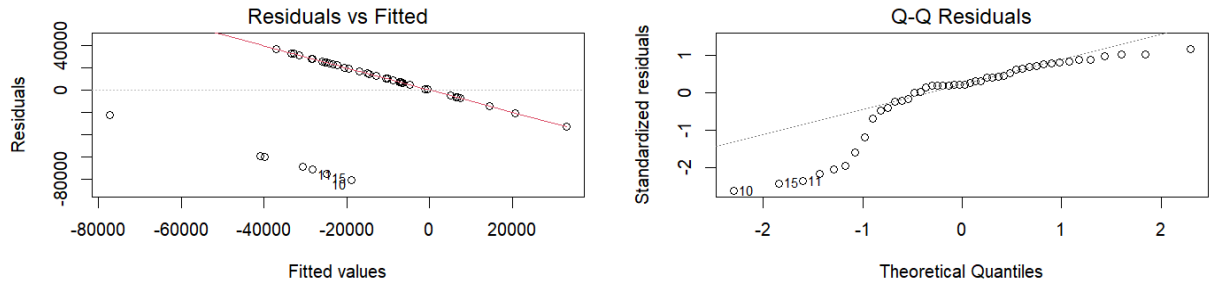

Figure 8. Diagnostic plots of the exploratory multiple linear regression for Drone and Satellite NDRE + NDVI on Nitrogen %. Residuals vs Fitted plot (left) indicates potential non-linearity due to the v-shape of the red line. Q-Q Residuals plot (right) indicates the values are normally distributed. Points 10, 11, and 15 are identified as potential outliers in both plots.

To evaluate the influence of Drone and Sentinel mean Normalized Difference Red Edge Index (NDRE) + Normalized Difference Vegetation Index (NDVI), three multiple linear models were used in R. The first model was a combination of Satellite NDRE & NDVI and Drone NDRE & NDVI (Combination) as the independent variables and Nitrogen % as the dependent variable.

The second model only assessed Satellite NDVI and Drone NDVI (NDVI). The third model only assessed Satellite NDRE and Drone NDRE (NDRE). Each model was assessed beforehand through the creation of diagnostic plots and vif (variance inflation factor) from the Car Package for R, of which all three models passed. Out of the three models, the combined model had the strongest indication of being correlated with Nitrogen %, with a P-Value of 0.01357, and the NDVI model having a P-Value of 0.01581. The P-Value of the NDRE model, 0.04079, indicates that NDRE-only models are weaker, but still acceptable, than NDVI only or a combination of NDRE and NDVI models. A BIC (Bayesian Information Criterion) test was performed to follow up our decision, which output the numbers: 0 (NDVI), 2.75 (NDVI+NDRE), 2.03 (NDRE). This indicates that the best-fit model is the NDVI only model, with the NDRE model being a potential alternative. Of the independent variables in the NDVI only model, the Sentinel (Satellite) Mean NDVI's P-value indicates that it is highly related with dependent variable, Nitrogen %, with the Drone mean NDVI's value indicating it is highly likely to be unrelated to the dependent variable.

Polynomial Regression Analysis

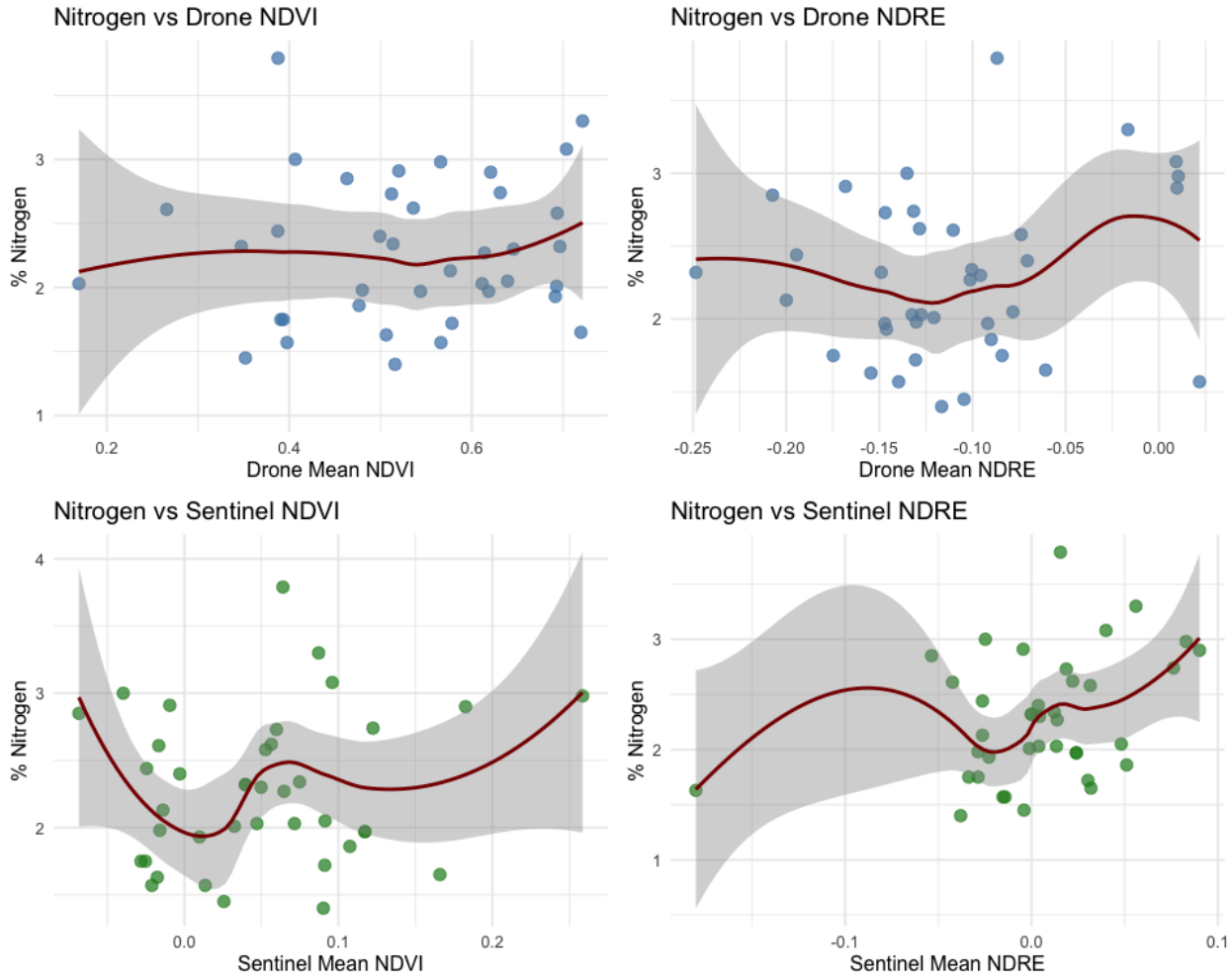

Figure 9. Exploratory scatter plots showing the relationship between kelp and nitrogen concentration (%N) and remote sensing indices. Blue points represent drone imagery, green points represent Sentinel satellite imagery. Red lines show LOESS smoothing curves with 95% confidence intervals.

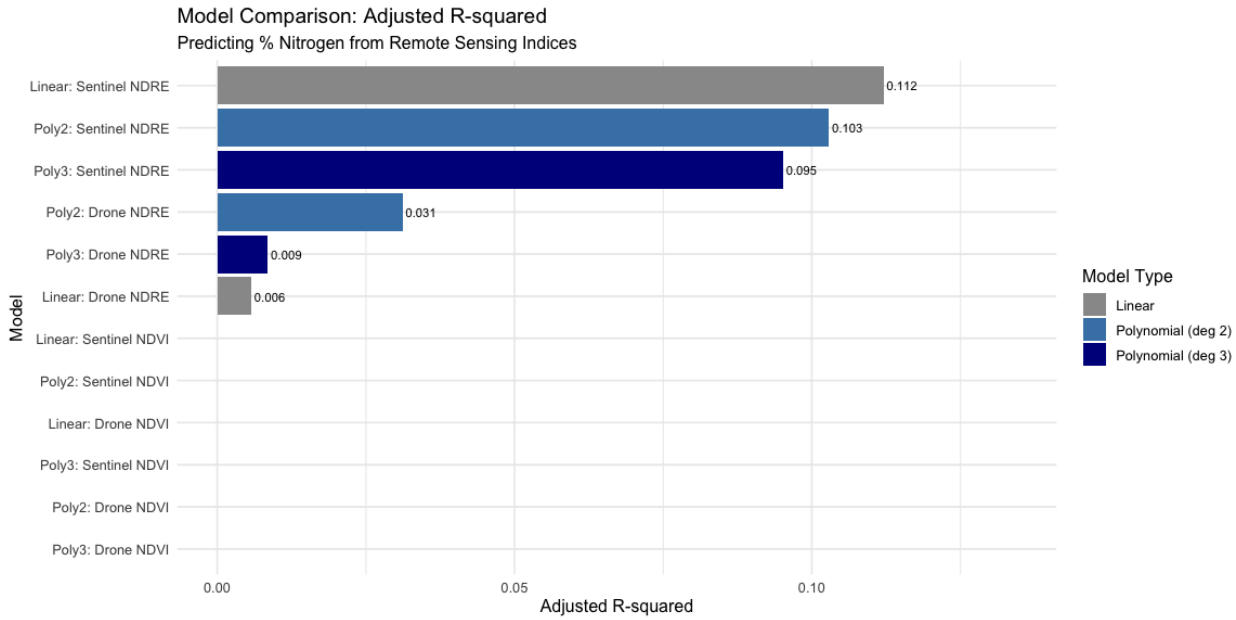

Figure 10. Model comparison showing adjusted R^2 values for linear, quadratic (degree 2), and cubic (degree 3) polynomial regression models predicting kelp nitrogen concentration from remote sensing indices (n = 39). Linear regression with Sentinel NDRE achieved the highest adjusted R^2 (0.112), followed by quadratic polynomial models using Drone NDRE (0.103) and Sentinel NDRE (0.095). NDRE-based models consistently outperformed NDVI-based models across all model types.

To evaluate whether non-linear relationships exist between remotely sensed vegetation indices and kelp nitrogen concentration, we compared polynomial regression models. We tested four predictors: Normalized Difference Vegetation Index (NDVI) and Normalized Difference Red Edge Index (NDRE) derived from both drone and Sentinel-2 satellite imagery. For each predictor, we fit three model types: linear regression, quadratic polynomial (degree 2), and cubic polynomial (degree 3), resulting in 12 single-predictor models. After removing observations with missing values, our final sample size was 39 observations. Model performance was evaluated using adjusted R^2, which accounts for model complexity, and statistical significance was assessed at $\alpha = 0.05$.

Linear regression with Sentinel NDRE emerged as the best-performing model (adjusted R^2 = 0.112), explaining approximately 11% of the variance in nitrogen concentration. Polynomial models did not improve upon the linear model; in fact, adjusted R^2 values decreased slightly for quadratic (0.103) and cubic (0.095) models due to overfitting penalties. This indicates that

the relationship between Sentinel NDRE and nitrogen is linear rather than curved. Across all model types, NDRE consistently outperformed NDVI as a predictor of nitrogen concentration, with all NDVI-based models showing near-zero or negative adjusted R^2 values.

Cubic polynomial models did not improve upon quadratic or linear models, with adjusted R^2 values decreasing due to overfitting penalties. This confirms that simpler models are sufficient for these data. Across all model types, NDRE consistently outperformed NDVI as a predictor of nitrogen concentration, with all top-performing models using NDRE indices.

The best-performing model explains approximately 11% of the variance in nitrogen concentration. While this represents a substantial improvement over initial analyses, a significant portion of variance remains unexplained. Additionally, polynomial regression requires pre-specifying the degree of the polynomial, which may not optimally capture complex non-linear relationships in ecological data. To address this limitation, we are also exploring Generalized Additive Models (GAMs), which allow the data to determine the shape of the relationship through smooth functions rather than fixed polynomial terms. GAMs offer greater flexibility in modeling non-linear relationships and may better capture the underlying patterns between remote sensing indices and kelp nitrogen concentration.

Drone vs. Satellite NDRE and NDVI Scatter Plots

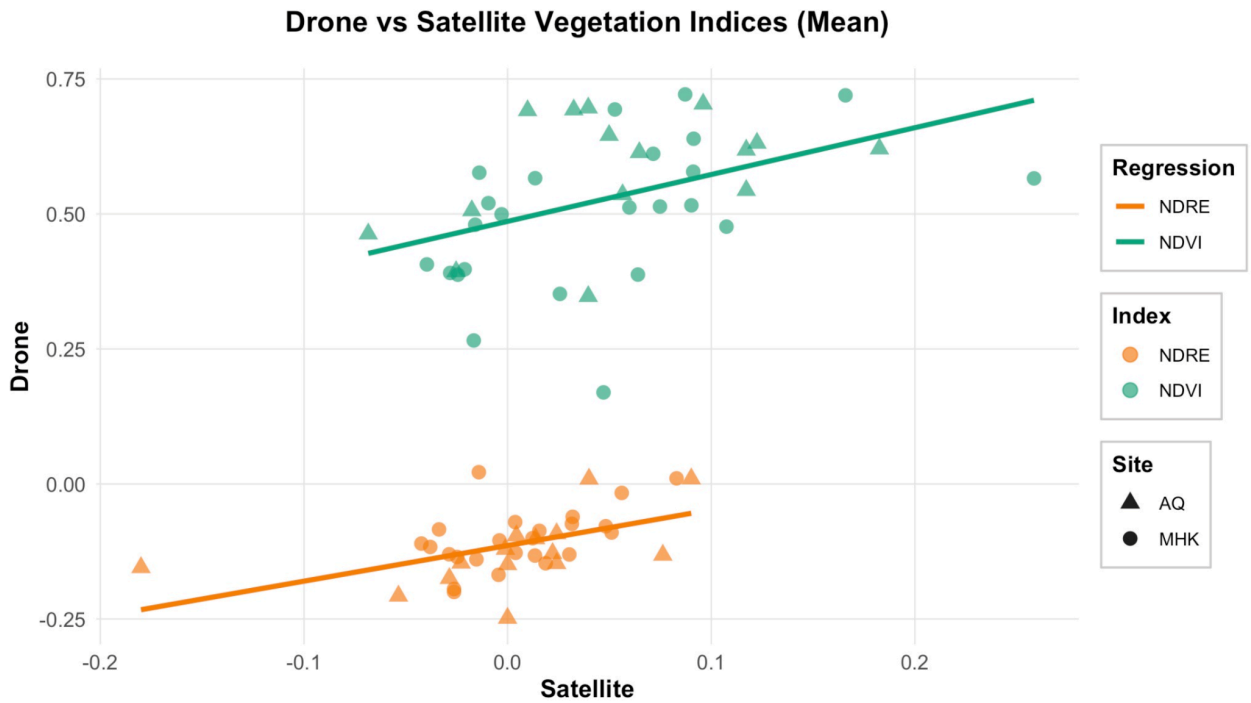

Figure 11. Comparison of mean vegetation indices between drone and satellite remote sensing methods. NDVI measurements (green points) show strong agreement between sites,

with drone values closely tracking satellite values across the full range of measurements. NDRE measurements (orange points) show moderate agreement, though both indices exhibit consistent positive relationships. Circles represent Mohawk site (MHK) and triangles represent Arroyo Quemado site (AQ). Overall, both sites capture similar patterns in NDVI and NDRE, with NDVI showing more consistent agreement between remote sensing methods than NDRE.

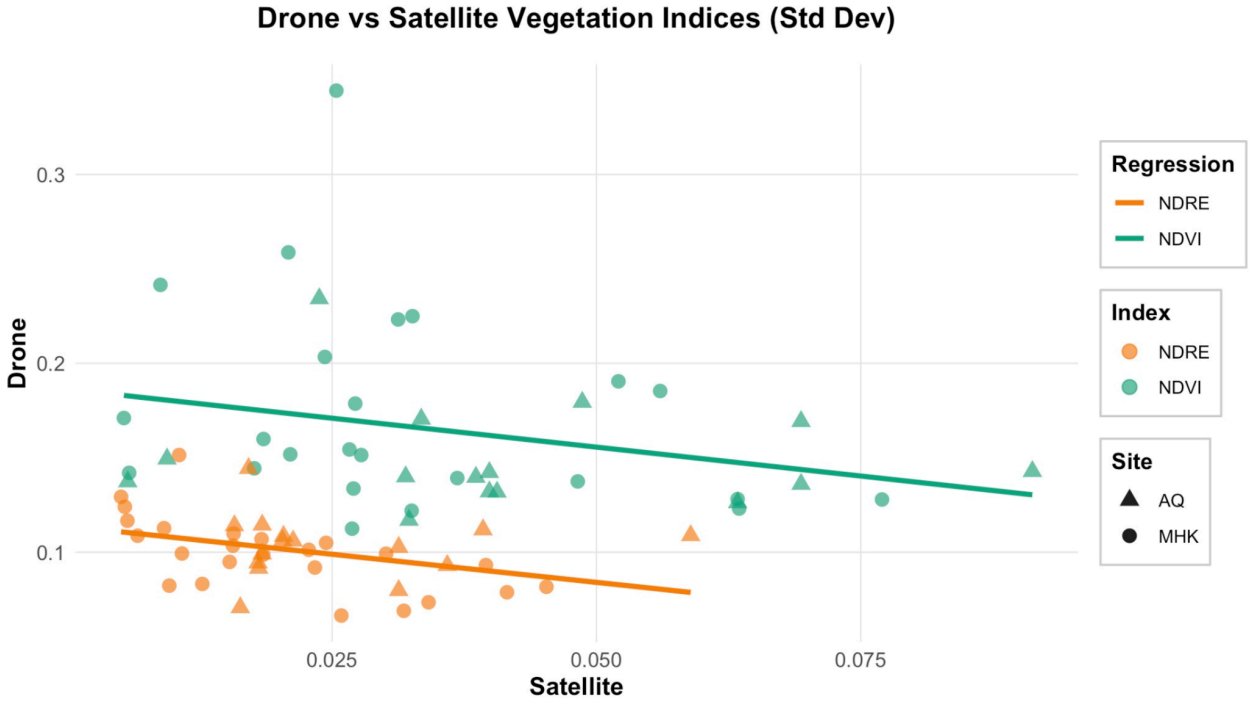

Figure 12. Comparison of standard deviation in vegetation indices between drone and satellite remote sensing methods. Drone measurements consistently show higher spatial variability than satellite measurements for both NDVI (green points) and NDRE (orange points), with an inverse relationship where lower satellite variability corresponds to higher drone variability. Circles represent Mohawk site (MHK) and triangles represent Arroyo Quemado site (AQ).

II. Workflow 1: Drone Classification

1. Import drone image into ArcGIS Pro project
2. In the contents menu, right click the image name and go to “Symbology” Change to RGB for better visualization:
   - Change red to Band 6
   - Change green to Band 4
   - Change blue to Band 2
3. Use “Add Data” to important the corresponding site box shapefile (either MHK_BOX or AQ_BOX)
4. Use the “Clip Raster” tool and input the following field selections before clicking “Run”:
   - Input Raster: site image

    - Output Extent: site box
    - Check the box for "use input features for clipping geometry"
5. Search "NDVI" and select the clipped image. Click "OK" after inputting the correct bands below. The range after running "NDVI" should be between -1 and 1
    - Visible band: Band 6
    - IR band: Band 10
    - Check the box for "scientific output"
6. Click on the NDVI layer name and then click "Imagery" in the top menu bar. Navigate to "Classification Tools" > "Training Sample Manager"
    - Click "Create New Schema"
    - Right click "New Schema" and hit "add new class"
    - Assign the following values:
        - Kelp = 1
        - Water = 2
        - Junk = 3
    - Use the "Polygon" tool to create 10 representative polygon areas for each class (kelp, water, junk)
    - Click "Save As" and navigate to the appropriate "SITE_DATE" folder to save this schema as "SITE_DATE_training"
7. Click on the name of the NDVI layer and then click "Classification Tools" > "Classify" > "Select Random Trees", then select the training data. Leave the default settings. Click the folder icon next to the output classified dataset and navigate to the SITE_DATE folder and save the output as "SITE_DATE_class.tif"
8. Change 'junk' and 'water' symbology to no color in the output and review the accuracy of the kelp classification
    - If it requires only minimal manual editing, proceed to next steps
    - If not, re-run using an order of magnitude higher values for the Random Trees parameters in Step 7 or try increasing the number of training polygons in Step 6
9. If manual editing is needed, select the classified output layer and click on "Imagery" > "Pixel Editor"
    - Change the current class to "Kelp" and the new class to "Water"
    - Click the "Reclassify" dropdown menu and select "Reclassify Region"
    - Select all pixels incorrectly classified as kelp
    - Double click to close the polygon
    - Click "Save" to save pixel edits
10. To clip the NDVI and 10-Band layers to kelp extent only, use the "Raster to Polygon" tool and set the following before hitting "Run":
    - Input raster: classified kelp layer
    - Select the "Class_Name" field
    - Output: SITE_DATE_Kelp_Polygons
    - Uncheck "simplify polygons" and "create multipart features" boxes

11. To select all non-kelp polygons, right click the new kelp polygon layer and click "Attribute table" > "Select by Attribute" then set the dropdown fields as follows before clicking "Apply" and "OK":
    - Row 1: "Where 'Class_Name' is equal to 'Water'"
    - Row 2: "OR where 'Class_Name' is equal to 'Junk'"
12. In the attribute table click "Delete" then save edits and close the attribute table
13. Use the "Zonal Statistics as Table" tool with the following field selections before clicking "Run":
    - Input Feature Zone Data: kelp polygons
    - Zone Field: ID
    - Input Raster: NDVI Clip raster
    - Output table: SITE_DATE_NDVI_Kelp_Polygons
    - Statistics Type: Mean
14. Right click the Kelp Polygons layer and click "Joins and Relates" > "Add Join" then set the fields as follows before hitting "OK":
    - Input Table: kelp polygons
    - Input Field: ID
    - Join Table: NDVI statistics table
    - Join Field: ID
    - Uncheck the "keep all input records" box
15. Repeat Steps 10–14 to summarize the 10-band image to the kelp polygons to enable calculations of other indices in addition to NDVI
    - Input raster: SITE_DATE_Clip layer
    - Feature Mask Data: kelp polygons
    - The output name: SITE_DATE_10BAND_Kelp_Polygons
    - Extraction Area: Inside
    - Click "Run"

III. Workflow 2: Analysis of Spectral Drone Indices

1. Use the "Zonal Statistics as Table" tool with the following field selections then click "Run":
    - Feature Zone Data: kelp polygon layer
    - Zone Field: Class_Name
    - Input Value Raster: NDVI layer
    - Output Table Name: SITE_DATE_Drone_NDVI_KELP
    - Statistics Type: All
2. To calculate the Normalized Difference Red Edge (NDRE), open the "Band Arithmetic" tool and select the original raster (SITE_DATE.tif) with the following field selections:
    - Method: User Defined
    - Band Indexes: (B10 – B8) / (B10 + B8)
3. Use the "Clip" tool to trim the resulting NDRE layer to the extent of the kelp polygons
4. Repeat Step 1 to calculate NDRE zonal statistics for the kelp polygons

5. Compile results in an Excel tracking sheet with the following columns: SITE, DATE, % carbon (LTER), % Nitrogen (LTER), C:N ratio (calculated as C/N), Drone mean NDVI, and Drone mean NDRE

IV. Workflow 1: Satellite Classification

1. Add the 10 meter Band 8 and the 20 meter Bands 2, 3, 4, 5, 6, 7, and 8A to a new ArcGIS Pro project named *SITE_DATE_Sentinel.*
2. *To analyze all bands at 20 meter resolution, resample any 10 meter bands using the Resample Tool: I*nput raster: 10 meter band.
    - Output folder: SITE_DATE_BAND_Resample.tif
    - X and Y output cell size: to 20 meter
    - Resampling technique: Bilinear
3. Use the Composite Bands Tool to combine all eight 20 meter bands (2, 3, 4, 5, 6, 7, 8, 8A):
    - Reorder the bands: 2, 3, 4, 5, 6, 7, 8, 8A
    - Output raster: SITE_DATE_CompositeBand
    - Click "Run"
4. Right-click the composite layer, select Symbology, and assign:
    - Red = Band 3
    - Green = Band 2
    - Blue = Band 1
5. Add the Site Box shapefile to the project
6. Clip the composite raster to the Site Box boundary using the Clip Raster Tool
7. Use the NDVI Tool to generate an NDVI raster:
    - Input: composite raster
    - Respective inputs: Band 3 (Red) and Band 7 (NIR)
    - Check "Scientific Output"
    - Click "Run
8. Use the NDVI raster to classify kelp presence following the same approach used for the drone imagery. Then follow steps 6 through 12 from drone imagery workflow 1.
9. Clip the composite band by the classified kelp raster to generate an 8-band layer displaying only the kelp coverage, which will be used to calculate and summarize spectral indices specific to the kelp canopy.

V. Workflow 2: Analysis of Spectral Satellite Indices

1. Open the Site_Date_Sentinenl ArcGIS file (from workflow 1)
2. Use Zonal Statistics as a Table and set the fields as follows:
    - Feature Zone Data: kelp polygon
    - Zone Field: Class_Name
    - Input Value Raster: NDVI raster
    - Statistics type: All
    - Output Table Name: SITE_DATE_Sentinel_NDVI_Kelp

3. Use Raster Calculator to create a NDRE layer following this example formula:
    - ("AQ_20230623_Resample" - "T10SGD_20230625T183921_B05_20m.jp2")/("AQ_20230623_Resample" + "T10SGD_20230625T183921_B05_20m.jp2")
    - Output Layer Name: SITE_DATE_Sentinel_NDRE.tif
4. Use Clip by Raster to clip the NDRE layer by the kelp polygons
5. Repeat step 2 using the clipped NDRE layer as the input value raster (replacing NDVI)
6. Open the attribute tables and add the Sentinel mean NDVI and Sentinel mean NDRE to the same spreadsheet used in Drone Workflow 2

VI.Literature Synthesis

Table 2. Remote Sensing Kelp Literature Synthesis.

Research Title	Sensor(s)	Bands	Time series (Y/N)	Diver data (Y/N)	Model (Y/N)	Kelp indices/ attributes	Species	Spatial scale	Citation
A High-Resolution Global Map of Giant Kelp (Macrocystis pyrifera) Forests and Intertidal Green Algae (Ulvophyceae) with Sentinel-2 Imagery	Satellite	Visible (blue, green, red), Red-Edge, NIR	Y	N	Y	Floating Algae Index (FAI), NDVI, and Kelp Difference (KD)	Giant Kelp	Global	Mora-Soto, A., Palacios, M., Macaya, E. C., Gómez, I., Huovinen, P., Pérez-Matus, A., Young, M., Golding, N., Toro, M., Yaqub, M., & Macias-Fauria, M. (2020). A High-Resolution Global Map of Giant Kelp (Macrocystis pyrifera) Forests and Intertidal Green Algae (Ulvophyceae) with Sentinel-2 Imagery. Remote Sensing, 12(4), 694. https://doi.org/10.3390/rs12040694
A Multi-Satellite Mapping Framework for Floating Kelp Forests	Satellite	Near-infrared	N	Y	Y	Aerial extent	Giant, Bull Kelp	Local	Gendall, L., Schroeder, S. B., Wills, P., Hessing-Lewis, M., & Costa, M. (2023). A Multi-Satellite Mapping Framework for Floating Kelp Forests. Remote Sensing, 15(5), 1276. https://doi.org/10.3390/rs15051276
AI-powered global interactive map	Aerial survey, other	Visible (blue, green, red), Red-Edge, and NIR	Y	N	Y	Kelp Canopy biomass	Not specified	Global	Kelp Sentinel. (n.d.). Kelp Sentinel Map. Coastal Carbon. Retrieved February 12, 2026, from https://kelpsentinel.coastalcarbon.ai/map

Artificial intelligence convolutional neural networks map giant kelp forests from satellite imagery	Satellite, other	Near-Infrared and Visible (red and green)	Y	N	Y	Canopy cover area across time	Giant Kelp	Regional	Marquez, L., Fragkopoulou, E., Cavanaugh, K.C. et al. Artificial intelligence convolutional neural networks map giant kelp forests from satellite imagery. Sci Rep 12, 22196 (2022). https://doi.org/10.1038/s41598-022-26439-w
BiogeoscienceslabOxford/kelp_forests	Satellite	Not specified	Y	N	N	NDVI, FAI, KD	Giant kelp	Global	Mora-Soto, A., Palacios, M., Macaya, E. C., Gómez, I., Huovinen, P., Pérez-Matus, A., Young, M., Golding, N., Toro, M., Yaqub, M., & Macias-Fauria, M. (2020). A high-resolution global map of giant kelp (Macrocystis pyrifera) forests and intertidal green algae (Ulvophyceae) with Sentinel-2 imagery. Remote Sensing, 12(4), 694.
Biomass estimations of cultivated kelp using underwater RGB images from a mini-ROV and computer vision approaches	UAV, aerial survey	Not specified	N	N	Y	Y	Sugar Kelp	Local	Overrein MM, Tinn P, Aldridge D, Johnsen G and Fragoso GM (2024) Biomass estimations of cultivated kelp using underwater RGB images from a mini-ROV and computer vision approaches. Front. Mar. Sci. 11:1324075. doi: 10.3389/fmars.2024.1324075
Branching Algorithm to Identify Bottom Habitat in the Optically Complex Coastal Waters of Atlantic Canada Using Sentinel-2 Satellite Imagery	Satellite	Visible (red, green, blue) and NIR	N	N	Y	NDVI	Not specified	Regional	Wilson KL, Wong MC and Devred E (2020) Branching Algorithm to Identify Bottom Habitat in the Optically Complex Coastal Waters of Atlantic Canada Using Sentinel-2 Satellite Imagery. Front. Environ. Sci. 8:579856. doi: 10.3389/fenvs.2020.579856

CubeSats show persistence of bull kelp refugia amidst a regional collapse in California	UAV, satellite	Visible (blue, green, red) and NIR	Y	N	Y	Kelp canopy extent, canopy presence/absence, canopy persistence, and refugia location and area relative to pre-collapse baseline	Bull kelp	Regional	Cavanaugh, K. C., Cavanaugh, K. C., Pawlak, C. C., Bell, T. W., & Saccomanno, V. R. (2023). CubeSats show persistence of bull kelp refugia amidst a regional collapse in California. Remote Sensing of Environment, 290, 113521. https://doi.org/10.1016/j.rse.2023.113521
Effect of Tides and Currents on UAV-Based Detection of Giant Kelp Canopy	UAV	Visible (red, green, blue)	Y	N	Y	Canopy area, canopy classification accuracy, and intra-seasonal/annual canopy variability	Giant kelp	Local	Cavanaugh, K. C. (2020). Effect of tides and currents on UAV-based detection of giant kelp canopy [Master's thesis, University of California, Los Angeles]. ProQuest Dissertations & Theses. https://www.proquest.com/docview/2420651766
Enhancing kelp forest detection in remote sensing images using crowdsourced labels with Mixed Vision Transformers and ConvNeXt segmentation models	Satellite, other	ShortWave InfraRed 1 (SWIR1), NIR, Visible (red and green)	Y	N	Y	Canopy presence/extent	Not specified	National	Junying Gan, Wenchao Xu, Hantian Chen, Zhen Chen, Zhenxin Zhuang & Huicong Li. (2025) ECL-ConvNeXt: An Ensemble Strategy Combining ConvNeXt and Contrastive Learning for Facial Beauty Prediction. Electronics 14:19, pages 3777.
Evaluation of remote sensing techniques for monitoring giant kelp populations	Ssatellite, aerial survey	NIR, Visible (green and blue)	N	N	Y	Canopy area/kelp biomass	Giant kelp	Regional	Deysher, L.E. Evaluation of remote sensing techniques for monitoring giant kelp populations. Hydrobiologia 260, 307–312 (1993). https://doi.org/10.1007/BF00049033

Kelp Patch-Specific Characteristics Limit Detection Capability of Rapid Survey Method for Determining Canopy Biomass Using an Unmanned Aerial Vehicle	UAV	Visible (blue, green, and red), Red-Edge, and NIR	N	Y	Y	Canopy biomass, kelp density, blade length, bulb diameter, sub-bulb diameter, and number of blades/fronds	Bull Kelp, Giant Kelp	Regional	McPherson ML and Kudela RM (2022) Kelp Patch-Specific Characteristics Limit Detection Capability of Rapid Survey Method for Determining Canopy Biomass Using an Unmanned Aerial Vehicle. Front. Environ. Sci. 10:690963. doi: 10.3389/fenvs.2022.690963
Kelp Tracker 2.0	UAV, satellite	Visible (red, green, blue) and NIR	Y	Y	Y	Canopy area, density, floating kelp extent, color index	Giant Kelp	Regional	Survey123 for ArcGIS. (n.d.). Kelp Tracker 2.0 [Online survey]. Survey123 for ArcGIS. https://survey123.arcgis.com/share/43e1ec88fd154b7ab21d67bc3f9e38f6
KelpGeoMod; DEVELOPING A DATA PIPELINE FOR KELP FOREST MODELING	UAV	Not specified	Y	Y	Y	Kelp occurrence, nitrite + nitrate, phosphate, and depth	Giant kelp	Local	Egg, E., French, J., Patrón, J., & Windschitl, E. (2023). Developing a data pipeline for kelp forest modeling. https://github.com/kelpGeoMod/kelpGeoMod-capstone-project.
Machine learning classification of intertidal macroalgae using UAV imagery and topographical indexes	UAV	Visible (red, green, blue)	N	N	Y	Macroalgae assemblages	Furbelows	Regional	Martínez Movilla, A., Rodríguez Somoza, J. L., and Martínez Sánchez, J.: Machine learning classification of intertidal macroalgae using UAV imagery and topographical indexes, Int. Arch. Photogramm. Remote Sens. Spatial Inf. Sci., XLVIII-4/W11-2024, 73–80, https://doi.org/10.5194/isprs-archives-XLVIII-4-W11-2024-73-2024, 2024.

MAPP KELP MONITORING METHODS 2021	UAV, other	NA	N	N	N	Kelp bed extent/perimeter, kelp density, stipe diameter, frond counts, bulb counts, bryozoan coverage	Giant kelp and bull kelp	Local to regional	Thompson, M. (2021). MaPP kelp monitoring protocol. Marine Plan Partnership for the North Pacific Coast. https://mappocean.org/wp-content/uploads/2021/07/MaPP_Kelp_Monitoring_Methods_2021.pdf
Mapping bull kelp canopy in northern California using Landsat to enable long-term monitoring	Satellite, aerial survey	Visible (blue, green, red) and NIR	Y	N	Y	Multiple endmember spectral mixture analysis and canopy area/biomass	Bull kelp	Local	Dennis J.I. Finger, Meredith L. McPherson, Henry F. Houskeeper, Raphael M. Kudela, Mapping bull kelp canopy in northern California using Landsat to enable long-term monitoring, Remote Sensing of Environment, 2021, https://doi.org/10.1016/j.rse.2020.112243.
Method development for mapping kelp using drones and satellite images: Results from the KELPMAP-Vega project	UAV, satellite	Visible (blue, green, red, dark red), IR, NIR	N	Y	Y	Kelp forest extent/area, habitat classification, brown algae percent cover, and kelp biomass estimates	Norwegian kelp	Local to regional	Gundersen, H., Hancke, K., Salberg, A. B., Poulsen, R. N., Buls, T., Liu, I. Y., Ghareeb, M., Christie, H. C., Kile, M. R., Bekkby, T., Arvidsson, K. S., & Kvile, K. Ø. (2024). Method development for mapping kelp using drones and satellite images: Results from the KELPMAP-Vega project. Norwegian Institute for Water Research (NIVA). NIVA-rapport.
Proximal Sensing for Characterising Seaweed Aquaculture Crop Conditions: Optical	Aerial survey, UAV	Visual (red, green, blue)	N	N	Y	ice-ice disease	Giant kelp	Local	Alevizos, E., Nurdin, N., Aris, A., & Barillé, L. (2024). Proximal Sensing for Characterising Seaweed Aquaculture Crop Conditions: Optical Detection of Ice-Ice Disease. Remote Sensing, 16(18), 3502.

Detection of Ice-Ice Disease									https://doi.org/10.3390/rs16183502
Remote Sensing Tools for Mapping and Monitoring Kelp Forests along the West Coast	Satellite	NIR and Visible (red, green, blue)	Y	N	Y	Kelp canopy area, kelp canopy extent/cover, kelp canopy biomass, and canopy persistence	Bull kelp and giant kelp	Local	National Oceanic and Atmospheric Administration, Office of National Marine Sanctuaries. (2023). Remote sensing tools for mapping and monitoring kelp forests along the West Coast. U.S. Department of Commerce. https://sanctuaries.noaa.gov/science/conservation/mapping-and-monitoring-kelp-forests.html
Remote sensing: generation of long-term kelp bed data sets for evaluation of impacts of climatic variation	Satellite	NIR	Y	Y	Y	Kelp canopy area, fractional canopy cover, and kelp canopy biomass	Giant kelp and bull kelp	Regional	Hamilton, S. L., Bell, T. W., Watson, J. R., Grorud-Colvert, K. A., & Menge, B. A. (2020). Remote sensing: Generation of long-term kelp bed data sets for evaluation of impacts of climatic variation. Ecology, 101(7), e03031. https://doi.org/10.1002/ecy.3031
SKeMa: Satellite-based Kelp Mapping	Satellite	Visible (red, green, blue) and NIR	Y	N	Y	Kelp canopy extent/area, kelp forest persistence (spatial and temporal), kelp distribution, and kelp resilience	Giant kelp and bull kelp	Regional	SPECTRAL Remote Sensing Laboratory, University of Victoria. (n.d.). Kelp: Spatial-temporal kelp dynamics. Retrieved from https://uvicspectral.com/kelp
The effects of kelp canopy submersion on the remote sensing of	UAV	Visible (red, blue, green),	N	N	Y	NDVI, NDRE, kelp difference (KD), and	Giant kelp and bull kelp	Local	Timmer, B. D. (2022). The effects of kelp canopy submersion on the remote sensing of surface-canopy forming kelps [Master's thesis, University of Victoria].

surface-canopy forming kelps		Red-edge, and NIR				above-water reflectance			
The Utility of Satellites and Autonomous Remote Sensing Platforms for Monitoring Offshore Aquaculture Farms: A Case Study for Canopy Forming Kelps	Satellite, aerial survey, other	Visible (blue, green, red) Red-edge, and NIR	Y	Y	Y	Canopy area, biomass, and tissue nitrogen content	Giant kelp	Local	Bell TW, Nidzieko NJ, Siegel DA, Miller RJ, Cavanaugh KC, Nelson NB, Reed DC, Fedorov D, Moran C, Snyder JN, Cavanaugh KC, Yorke CE and Griffith M (2020) The Utility of Satellites and Autonomous Remote Sensing Platforms for Monitoring Offshore Aquaculture Farms: A Case Study for Canopy Forming Kelps. Front. Mar. Sci. 7:520223. doi: 10.3389/fmars.2020.520223
Using unoccupied aerial vehicles to map and monitor changes in emergent kelp canopy after an ecological regime shift	UAV	Visible (red through blue)	Y	N	Y	Canopy area/extent	Not specified	Regional	Saccomanno, V. R., Bell, T., Pawlak, C., Stanley, C. K., Cavanaugh, K. C., Hohman, R., Klausmeyer, K. R., Cavanaugh, K., Nickels, A., & Hewerdine, W. (2022). Using unoccupied aerial vehicles to map and monitor changes in emergent kelp canopy after an ecological regime shift. Remote Sensing in Ecology and Conservation. https://doi.org/10.1002/rse2.295

Quantitative Assessment of Remote Sensing Capabilities to Improve Monitoring of Giant Kelp Condition

As authors of this Group Project report, we archive this report on the Bren School's website such that the results of our research are available for all to read. Our signatures on the document signify our joint responsibility to fulfill the archiving standards set by the Bren School of Environmental Science & Management.

_____ _____

Emilie Lenoir Date

_____ _____

Michelle Moreno Date

_____ _____

Charles O'Connor IV Date

_____ _____

Tanvi Shah Date

_____ _____

Danielle Turner Date

The Bren School of Environmental Science & Management produces professionals with unrivaled training in environmental science and management who will devote their unique skills to the diagnosis, assessment, mitigation, prevention, and remedy of the environmental problems of today and the future. A guiding principle of the Bren School is that the analysis of environmental problems requires quantitative training in more than one discipline and an awareness of the physical, biological, social, political, and economic consequences that arise from scientific or technological decisions.

The Group Project is required of all students in the Master of Environmental Science and Management (MESM) Program. The project is a year-long activity in which small groups of students conduct focused, interdisciplinary research on the scientific, management, and policy dimensions of a specific environmental issue. This Group Project Final Report is authored by MESM students and has been reviewed and approved by:

_____ _____

Faculty Advisor Date

Hunter Lenihan